Zeitschrift: IABSE publications = Mémoires AIPC = IVBH Abhandlungen
Band: 29 (1969)

Artikel: Seismic dynamic analyses of a railway bridge
Autor: Walpole, W.R. / Shepherd, R.
DOI: https://doi.org/10.5169/seals-22929

Nutzungsbedingungen
Die ETH-Bibliothek ist die Anbieterin der digitalisierten Zeitschriften auf E-Periodica. Sie besitzt keine Urheberrechte an den Zeitschriften und ist nicht verantwortlich für deren Inhalte. Die Rechte liegen in der Regel bei den Herausgebern beziehungsweise den externen Rechteinhabern. Das Veröffentlichen von Bildern in Print- und Online-Publikationen sowie auf Social Media-Kanälen oder Webseiten ist nur mit vorheriger Genehmigung der Rechteinhaber erlaubt. Mehr erfahren

Conditions d'utilisation
L'ETH Library est le fournisseur des revues numérisées. Elle ne détient aucun droit d'auteur sur les revues et n'est pas responsable de leur contenu. En règle générale, les droits sont détenus par les éditeurs ou les détenteurs de droits externes. La reproduction d'images dans des publications imprimées ou en ligne ainsi que sur des canaux de médias sociaux ou des sites web n'est autorisée qu'avec l'accord préalable des détenteurs des droits. En savoir plus

Terms of use
The ETH Library is the provider of the digitised journals. It does not own any copyrights to the journals and is not responsible for their content. The rights usually lie with the publishers or the external rights holders. Publishing images in print and online publications, as well as on social media channels or websites, is only permitted with the prior consent of the rights holders. Find out more

Download PDF: 09.02.2026

ETH-Bibliothek Zürich, E-Periodica, https://www.e-periodica.ch

Seismic Dynamic Analyses of a Railway Bridge

Analyse dynamique d'un pont de chemin de fer en fonction de mouvements sismiques

Erdbebenuntersuchungen einer Eisenbahnbrücke

W. R. WALPOLE
Assistant Engineer, Beca, Carter, Hollings & Ferner, Consulting Engineers, Wellington, New Zealand

R. SHEPHERD
Reader in Civil Engineering, Canterbury University, Christchurch, New Zealand

1. Introduction

This paper describes both elastic and elasto-plastic seismic dynamic analyses of a proposed design for a railway bridge for the New Zealand North Island Main Trunk. The structure consists of a continuous reinforced concrete deck beam of fourteen 40 feet spans, supported by single reinforced concrete cylindrical piers, except that three of the piers consist of two inclined cylindrical members, as shown in the elevations in Fig. 1. The bridge was designed so that, under a strong motion earthquake acting transversely to the deck, plastic hinges would form in the deck beam.

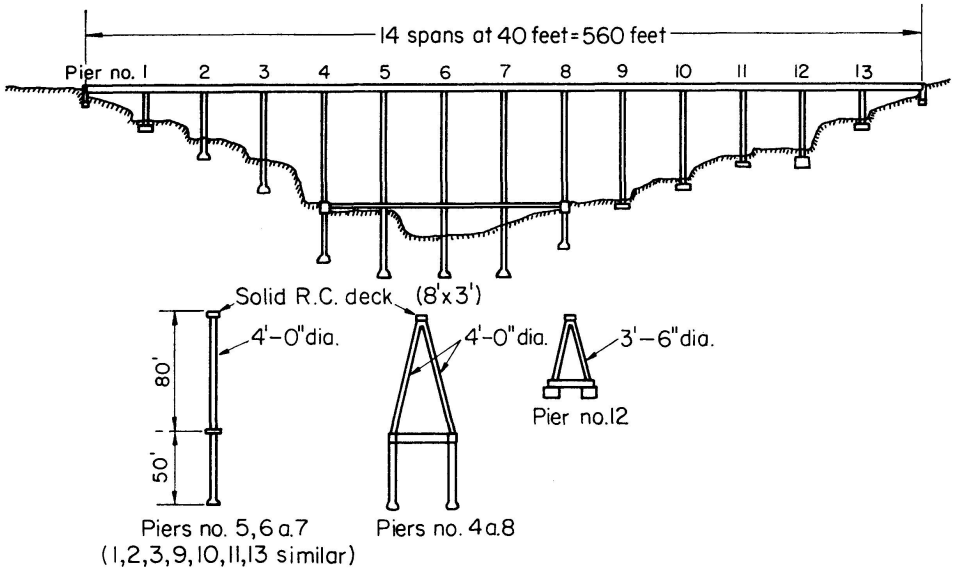

Fig. 1.

2. General Assumptions Adopted to Facilitate Analysis

It was assumed that the axial deformation in all beams and vertical piers, and rotations in the plane of the structure were negligible because there was no loading corresponding to these deformations. Shear deformations and joint size effects were neglected for simplicity. The pad footings were assumed to provide a pin joint and the belled piles to rigidly fix the piers a little below ground level. Axial and bending deformations were considered in the inclined piers which were assumed to be rigidly fixed at the tie beams at ground level. Fig. 2 shows the sixteen lateral co-ordinates used to define the displaced shape

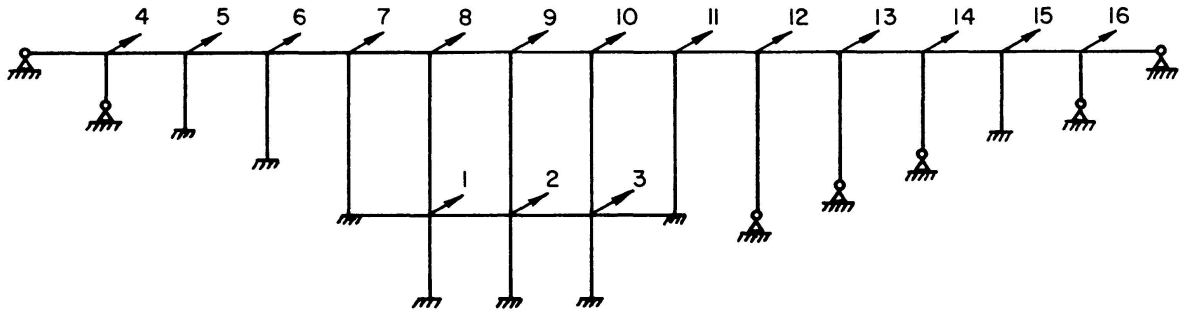

Fig. 2.

of the structure. There were also two rotations associated with each lateral displacement, one about the vertical pier axis and one about the deck beam axis. This means that when the equations of equilibrium for the structure are written it is necessary to consider the torsional stiffness of the beam and column members.

The weight of each beam was divided equally between adjacent columns and lumped at the joints with the column. Part of the weight of each column was lumped at the top of the column. This gave sixteen masses each associated with a lateral co-ordinate.

3. Elastic Analysis

The response of the structure to earthquake loading was predicted by calculating the normal mode properties and summing the response of each mode determined using a response spectrum [1].

The normal mode properties were determined by iteration of the lateral flexibility matrix which was determined by the inversion of the stiffness matrix. A computer program was written to assemble the stiffness matrix [2]. The assembly routine allows for the possibility of a hinge occurring at either end, and in addition for the effect of a torsional moment at both ends and for the inclined pier members (see Appendix).

After the stiffness matrix has been assembled and inverted, the lateral

flexibility matrix was formed by picking out the appropriate coefficients from the flexibility matrix.

The normal mode properties were found by iteration using a digital computer [2]. The values of the mass lumped at the co-ordinate points are given in Table 1. The maximum elastic response of the bridge was predicted by finding the response of each mode using Skinner's response curve [1] for 10% critical damping and taking the root mean square of the modal responses.

The normal mode properties and the predicted response are listed in Table 1. The notation of the lateral deformations used in Table 1 corresponds to that

Table 1. Normal Mode Properties

Mode 1

Frequency = 1.87 c.p.s. Period = 0.534
Amplification Factor = 0.62

Mass	Displacement Ratios	1 g Displacements inches	1 g Shears Kips
16	0.0314	0.0098	0.58
15	−0.0932	−0.0291	−1.92
14	−0.5204	−0.1624	−10.93
13	−0.8123	−0.2536	−18.45
12	−0.6162	−0.1923	−14.78
11	0.0219	0.0068	0.53
10	0.7236	0.2259	17.36
9	1.0000	0.3121	23.99
8	0.6820	0.2129	16.36
7	0.1086	0.0339	2.61
6	−0.1832	−0.0572	−3.97
5	−0.1936	−0.0604	−3.86
4	−0.0818	−0.0256	−1.53
3	0.0323	0.0101	0.77
2	0.0586	0.0183	1.44
1	0.0312	0.0098	0.75

Mode 2

Frequency = 2.36 Period = 0.424
Amplification Factor = 0.71

Mass	Displacement Ratios	1 g Displacements inches	1 g Shears Kips
16	−0.0379	−0.089	−8.4
15	0.1380	0.325	34.0
14	0.6978	1.644	175.5
13	1.0000	2.356	271.9
12	0.7035	1.657	202.0
11	0.2847	0.671	81.8
10	0.4747	1.118	136.3
9	0.7245	1.707	208.1
8	0.5504	1.296	158.1
7	0.0907	0.214	26.1
6	−0.1824	−0.430	−47.3
5	−0.2043	−0.481	−48.8
4	−0.0906	−0.213	−20.3
3	0.0210	0.050	6.0
2	0.0416	0.098	12.2
1	0.0237	0.056	6.8

Mode 3

Frequency = 3.165 Period = 0.316
Amplification Factor = 0.72

Mass	Displacement Ratios	1 g Displacements inches	1 g Shears Kips
16	−0.0006	−0.0010	−0.17
15	0.0049	0.0075	1.40
14	0.0198	0.0297	5.71
13	0.0227	0.0340	7.07
12	0.0166	0.0249	5.47
11	0.0491	0.0736	16.15
10	0.1472	0.2205	48.39
9	0.1606	0.2406	52.80
8	0.1064	0.1593	34.97
7	0.2792	0.4182	91.78
6	0.8608	1.2890	255.30
5	1.0000	1.4970	273.20
4	0.4881	0.7311	124.80
3	0.0039	0.0059	1.28
2	0.0050	0.0076	1.71
1	0.0012	0.0019	0.40

Predicted Elastic Response

Co-ordinate	Lumped Mass Kips	Displacement inches	Force Kips
16	164.9	0.064	6.0
15	183.9	0.232	24.3
14	187.7	1.177	125.5
13	202.9	1.688	194.4
12	214.3	1.188	144.5
11	214.3	0.482	59.5
10	214.3	0.826	104.0
9	214.3	1.246	154.1
8	214.3	0.942	116.0
7	214.3	0.341	69.2
6	193.4	0.986	188.5
5	178.2	1.141	201.5
4	166.8	0.553	91.9
3	213.2	0.036	4.4
2	218.9	0.071	8.9
1	213.2	0.040	4.9

shown in Fig. 2. The displaced shape of the deck beam in the first three modes is shown in Fig. 3.

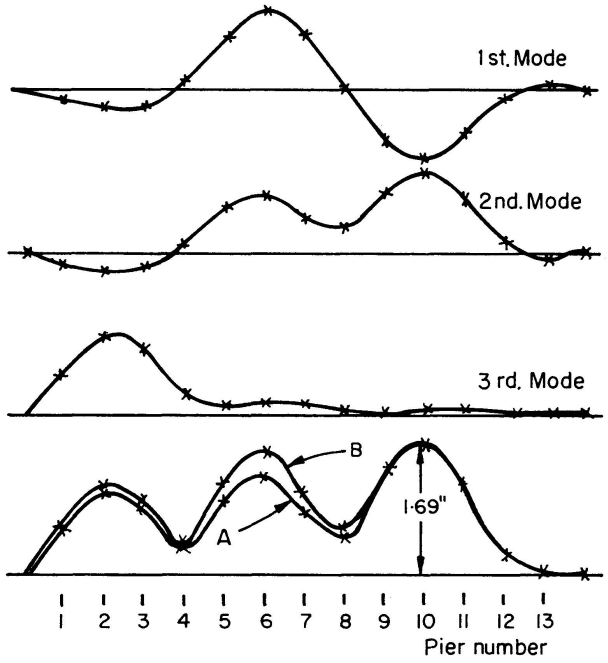

Fig. 3. Curve A: Predicted elastic response by R.M.S. Curve B: Response by direct integration.

The maximum response of the bridge to the North-South Component of the 1940 E. Centro earthquake was found by integrating the first three modal equations of motion and summing the response of each mode at the end of each step interval and also by integrating the sixteen equations of motion for the lumped masses. The two integrations give practically identical answers and are compared with the displacements found by the root mean square of the modal responses in Fig. 3.

The member actions associated with the maximum elastic displacements under the El Centro record were found by determining the statically equivalent forces required to produce these displacements. These forces were found by inverting the lateral flexibility matrix to give the lateral stiffness matrix and then multiplying this by the maximum lateral displacements. The rotations produced by these equivalent forces were found by multiplying the appropriate sub-matrix of the flexibility matrix by the forces.

The process then consists of the following steps:

$$\{P_{eq}\} = [K_{LAT}]\{\delta_{max}\},$$

where $\{\delta_{max}\}$ is a vector of the maximum lateral displacements,
$\{P_{eq}\}$ is the vector of equivalent lateral forces,
$[K_{LAT}]$ is the lateral stiffness matrix.

Then

$$\{\theta\} = [F_{12}]\{P_{eq}\},$$

where θ is the vector of rotations of the bridge,
F_{12} is a sub-matrix of the flexibility matrix, when it is partitioned so

that the terms associated with the rotations are separated from those associated with the displacements, as follows:

$$\begin{Bmatrix} \theta \\ \delta \end{Bmatrix} = \begin{bmatrix} F_{11} & F_{12} \\ F_{21} & F_{22} \end{bmatrix} \begin{Bmatrix} M \\ P \end{Bmatrix},$$

where δ is the vector of the lateral displacements,
M is a vector of applied moments, usually null,
P is a vector of the lateral forces,
F_{11}, F_{12}, F_{21} and F_{22} being sub-matrices of the flexibility matrix. F_{22} being the lateral flexibility matrix $[F_{LAT}]$.

Once the bridge deformations were established the individual member actions were found by setting up the member stiffness matrices and multiplying by the appropriate deformations.

The member actions caused by a code type loading, with lateral loads determined by using a seismic coefficient of 0.15 at the deck level and 0.05 at the tie beam level, were also found by using the specially developed computer programs. A factor of roughly 4.5 was needed to reduce the predicted elastic response to the code response [3]. The moments in the deck beam caused by the code-type loading are compared with the maximum moments assuming elastic response to the El Centro record and with the ultimate moments in Fig. 4.

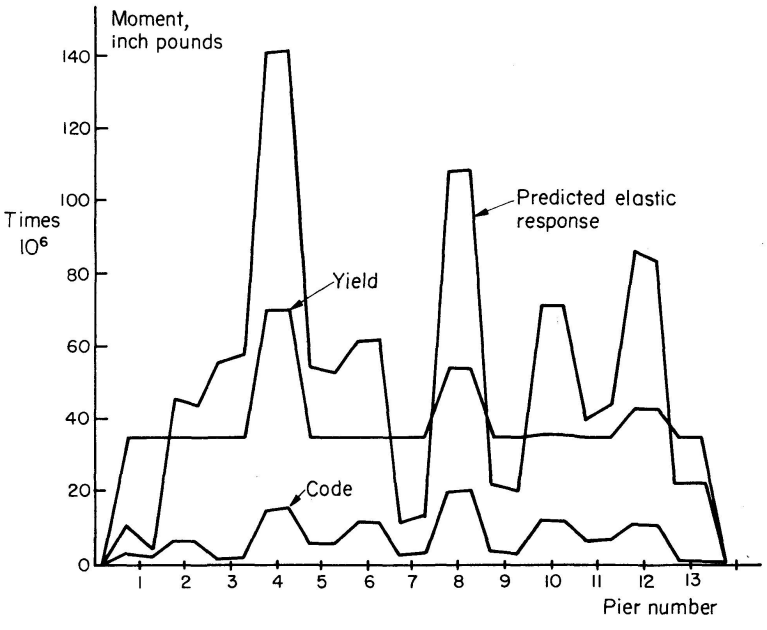

Fig. 4. Moments in deck beam.

4. Elasto-Plastic Analysis

A method similar to that developed by CLOUGH, BENUSKA and WILSON [4] was used [2] to determine the idealised elasto-plastic response of the bridge to strong-motion earthquake motion. A digital computer was employed to

directly integrate the equations of motion, the structure being allowed to respond in a linear elastic manner during each time increment. The non-linear behaviour was then obtained as a sequence of responses of successively differing systems.

A computer program was written to determine the elasto-plastic response of the bridge to the El Centro N-S record, assumed to be applied transversely to the structure. The program included provision for the structural members to behave in an idealised elasto-plastic manner (see fig. 5). The stiffness matrix assembly procedure incorporated the particular provisions referrred to in the elastic analysis section and detailed in the Appendix.

The bridge was analysed with this program initially keeping all the members

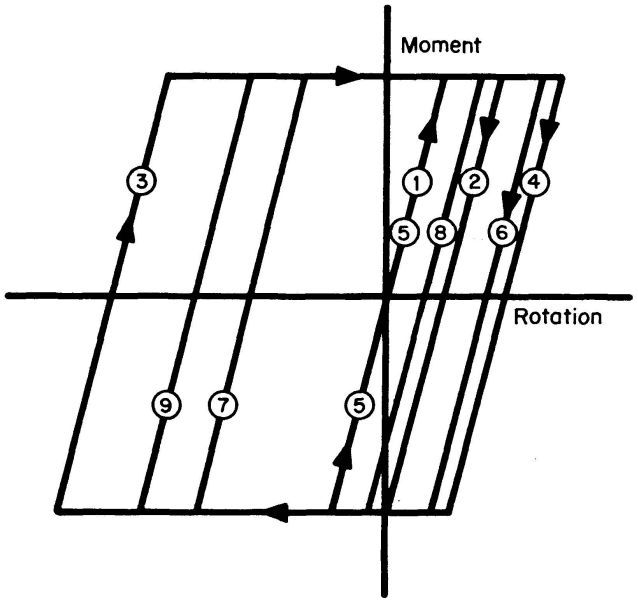

Fig. 5.

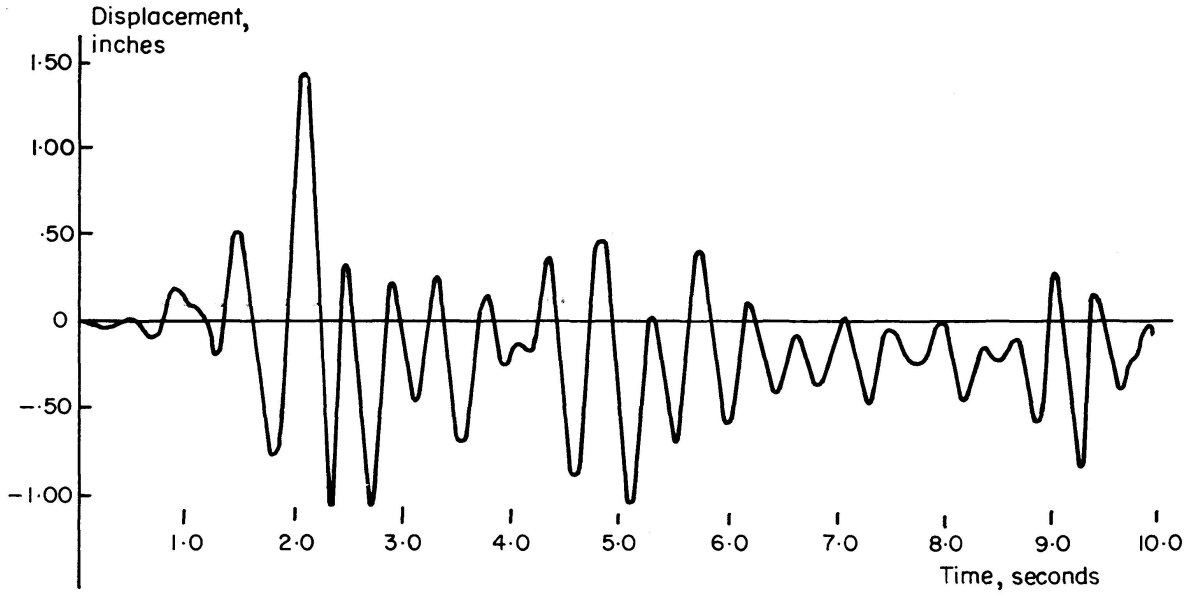

Fig. 6. Response of pier no. 10.

elastic by using high yield moments and it was found that this elastic response was practically identical to that found previously. The bridge was then analysed allowing plastic hinges to form in the deck beam by selecting more realistic ultimate moments.

The ultimate moments of the beams were assumed to be half the maximum moment reached assuming elastic behaviour, except that no beam was allowed to have a yield moment less than 35×10^6 in. lb., half the greatest ultimate moment. This procedure meant that the ultimate moments were set at approximately twice the moments caused by code loading. This is in line with current New Zealand practice.

The variation of the lateral displacement of pier number 10 with time is given in Fig. 6. (The pier numbers are given in Fig. 1.) The maximum dis-

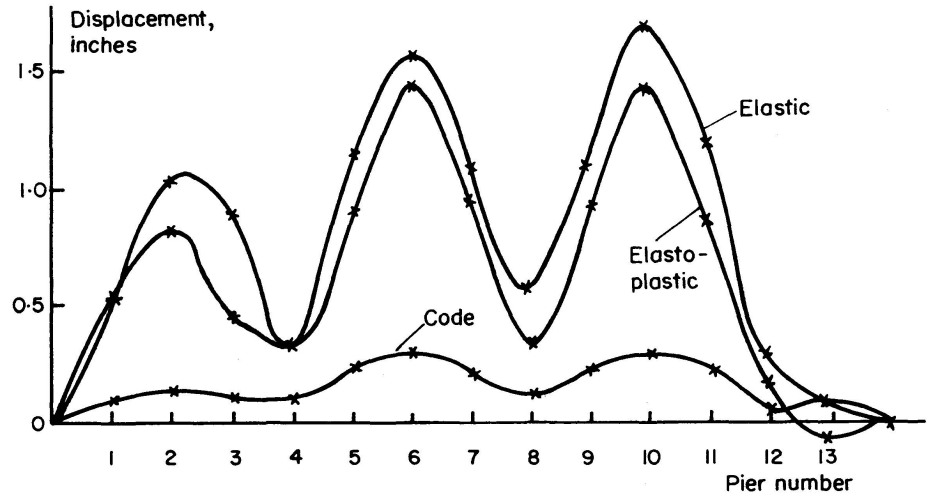

Fig. 7. Response of deck beam.

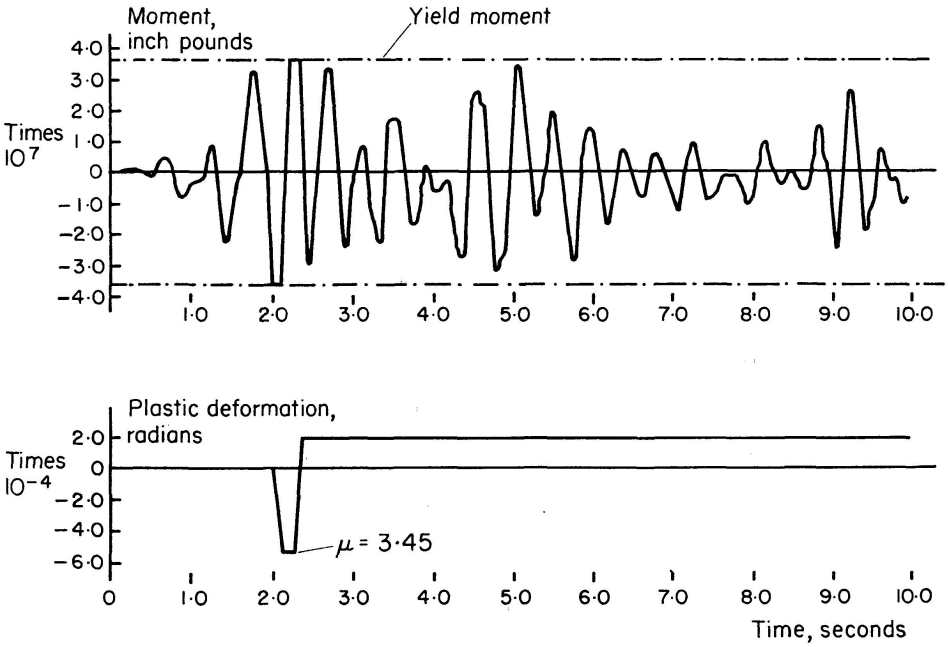

Fig. 8. Moment in deck beam between piers 9 and 10.

placements of the piers are compared with the maximum values assuming elastic behaviour and with the displaced shape caused by code loading in Fig. 7. It can be seen that the plastic action reduces the maximum displacements a little, but the displaced shape is essentially similar.

The variation of the bending moment with time at the end of a typical deck beam member, that between piers 9 and 10, is shown in Fig. 8, together with the growth of plastic deformation for the same section.

The plastic deformations for the deck beam are given in the form of the member ductility ratio in Fig. 9 and are compared with the ratio of the maximum moment assuming elastic behaviour to the ultimate moment for the same section. There is a definite tendency for the peaks in the moment ratio curve to be accentuated in the ductility ratio plot, particularly where there was a relatively large elastic deflection. The maximum ductility ratio was 4.67.

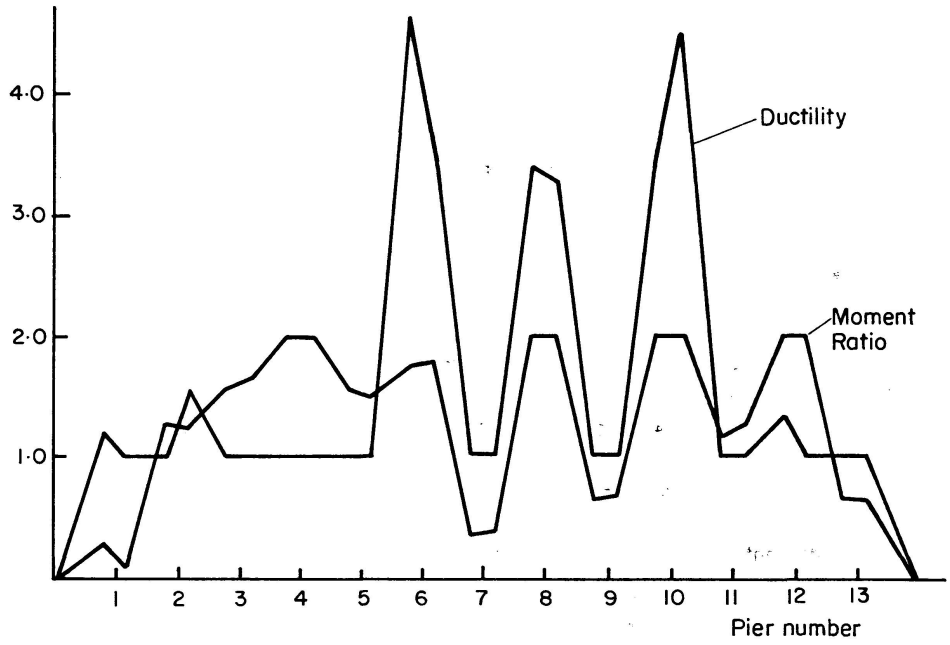

Fig. 9. Ductility required in deck beam.

5. Conclusions

It has been shown that for the bridge examined, designing the deck beam to yield at half the maximum seismic elastic moments gave satisfactory elasto-plastic behaviour. The elasto-plastic displacements were slightly less than those computed assuming elastic behaviour and the member ductilities were of reasonable magnitude with a maximum of 4.67.

6. Acknowledgements

The authors are indebted to J. P. Hollings, partner in Beca, Carter, Hollings and Ferner, Consulting Engineers of Wellington, New Zealand, and his clients,

New Zealand Railways for their interest in this work and particularly their permission to publish this paper.

The analysis procedures were developed by the first author as part of his Ph. D. studies, under the supervision of the second author.

Appendix: Particular Considerations Adopted in the Stiffness Matrix Assembly Routine

The configuration of the structure analysed necessitated the following particular considerations of the member equilibrium equations in order that a general stiffness matrix analysis approach could be used.

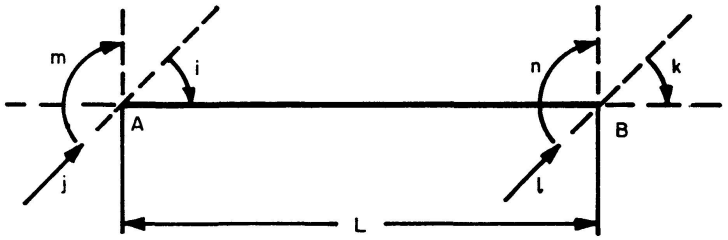

Fig. 10.

The equilibrium equations for a typical beam AB shown in Fig. 10 are given below where the letters in the diagram are used to distinguish actions and their corresponding deformations.

1. With no hinges present:

$$\begin{Bmatrix} M_i \\ F_j \\ M_k \\ F_l \\ M_m \\ M_n \end{Bmatrix} = \begin{bmatrix} \frac{4EI}{L} & \frac{6EI}{L^2} & \frac{2EI}{L} & -\frac{6EI}{L^2} & \cdot & \cdot \\ & \frac{12EI}{L^3} & \frac{6EI}{L^2} & -\frac{12EI}{L^3} & \cdot & \cdot \\ & & \frac{2EI}{L} & -\frac{6EI}{L^2} & \cdot & \cdot \\ & & & \frac{12EI}{L^3} & \cdot & \cdot \\ & & & & \frac{GJ}{L} & \frac{GJ}{L} \\ \text{symmetrical} & & & & & \frac{GJ}{L} \end{bmatrix} \begin{Bmatrix} \theta_i \\ \delta_j \\ \theta_k \\ \delta_l \\ \theta_m \\ \theta_n \end{Bmatrix}, \qquad \text{(a)}$$

where M denotes an action which is a bending moment,
F denotes an action which is a force,
θ denotes a deformation which is a rotation,
δ denotes a deformation which is a displacement.

Subscripts are used to distinguish individual action and deformations.

E is the Elastic Modulus.
G is the Shear Modulus.
I is the Second Moment of Area.
L is the Length.
J is the Polar Moment of Inertia of the Section.
$J = D^4/32$ for a circular section where D is the diameter.
$J = k_1 b^3 D$ for a rectangular section, b being the smaller side, D the larger side, k_1 being determined from tables prepared by TIMOSHENKO [5].

2. With a hinge at end A the equilibrium equations become:

$$\begin{Bmatrix} M_i \\ F_j \\ M_k \\ F_l \\ M_m \\ M_n \end{Bmatrix} = \begin{bmatrix} . & . & . & . & . & . \\ \frac{3EI}{L^3} & \frac{3EI}{L^2} & -\frac{3EI}{L^3} & . & . & \\ & \frac{3EI}{L} & -\frac{3EI}{L^2} & . & . & \\ & & \frac{3EI}{L^3} & . & . & \\ & & & \frac{GJ}{L} & -\frac{GJ}{L} & \\ \text{symmetrical} & & & & \frac{GJ}{L} & \end{bmatrix} \begin{Bmatrix} \theta_i \\ \delta_j \\ \theta_k \\ \delta_l \\ \theta_m \\ \theta_n \end{Bmatrix}. \qquad \text{(b)}$$

Where θ_i is the rotation about the vertical axis of joint A of the frame, as before, and not the rotation of end A of member AB.

The formation of a plastic hinge is assumed not to affect the torsional stiffness about the longitudinal axis of the member.

3. With a hinge at end B the equilibrium equations for the member AB become:

$$\begin{Bmatrix} M_i \\ F_j \\ M_k \\ F_l \\ M_m \\ M_n \end{Bmatrix} = \begin{bmatrix} \frac{3EI}{L} & \frac{3EI}{L^2} & . & -\frac{3EI}{L^2} & . & . \\ & \frac{3EI}{L^3} & . & -\frac{3EI}{L^3} & . & . \\ & & . & . & . & . \\ & & & \frac{3EI}{L^3} & . & . \\ & & & & \frac{GJ}{L} & -\frac{GJ}{L} \\ \text{symmetrical} & & & & & \frac{GJ}{L} \end{bmatrix} \begin{Bmatrix} \theta_i \\ \delta_j \\ \theta_k \\ \delta_l \\ \theta_m \\ \theta_n \end{Bmatrix}. \qquad \text{(c)}$$

4. With hinges at both ends A and B the equilibrium equations become:

$$\begin{Bmatrix} M_i \\ F_j \\ M_k \\ F_l \\ M_m \\ M_n \end{Bmatrix} = \begin{bmatrix} \cdot & \cdot & \cdot & \cdot & \cdot & \cdot \\ & \cdot & \cdot & \cdot & \cdot & \cdot \\ & & \cdot & \cdot & \cdot & \cdot \\ & & & \cdot & \cdot & \cdot \\ & & & & \frac{GJ}{L} & -\frac{GJ}{L} \\ & & \text{symmetrical} & & & \frac{GJ}{L} \end{bmatrix} \begin{Bmatrix} \theta_i \\ \delta_j \\ \theta_k \\ \delta_l \\ \theta_m \\ \theta_n \end{Bmatrix}. \tag{d}$$

The equilibrium equations for a typical column member CD shown in Fig. 11 are identical to (a) with no hinges present and identical to (b) with a hinge at the base.

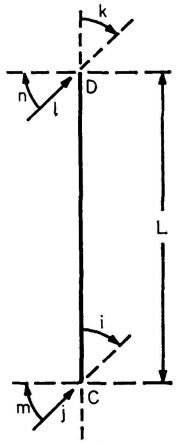

Fig. 11.

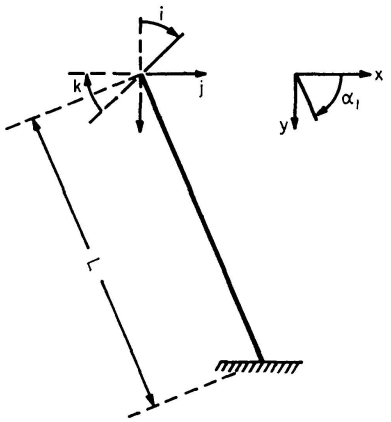

Fig. 12.

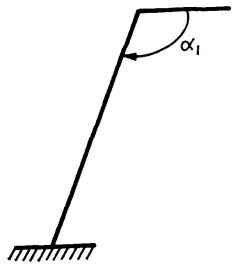

Fig. 13.

With the inclined members it is only necessary to consider the equilibrium of one joint as the other end is fully fixed. For a pier member inclined at angle α to the horizontal x axis (see fig. 12), there are three unknown deformations and the member equilibrium equations may be written:

$$\begin{Bmatrix} M_i \\ F_j \\ M_k \end{Bmatrix} = \begin{bmatrix} \frac{4EI}{L} & -S\frac{6EI}{L^2} & \cdot \\ -S\frac{6EI}{L^2} & \left(C^2\frac{EA}{L} + S^2\frac{12EI}{L^3}\right) & \cdot \\ \cdot & \cdot & S\frac{GJ}{L} \end{bmatrix} \begin{Bmatrix} \theta_i \\ \delta_j \\ \theta_k \end{Bmatrix},$$

where E, I, L and G, are as previously defined.

A is the cross sectional area and J is the Polar Moment of Inertia.

$$S = \sin \alpha,$$
$$C = \cos \alpha.$$

α is the angle measures to the x-axis, thus for the left-hand member, α, is obtuse (see fig. 13).

7. References

1. SKINNER, R. I. (1962): Handbook for Earthquake Generated Forces and Movements in Tall Buildings. Bulletin 166, Department of Scientific and Industrial Research, Wellington, New Zealand.
2. WALPOLE, W. R. (1968): The Response of Structures to Earthquake Loading. Unpublished Ph. D. Thesis, University of Canterbury, Christchurch, New Zealand.
3. — (1965): New Zealand Standard Model Building Bylaw. N.Z.S.S. 1900 chapter 8 "Basic Loads to be used in Design and their Method of Application". New Zealand Standards Institute, Wellington.
4. CLOUGH, R. W., BENUSKA, K. L., and WILSON, E. L. (1965): Inelastic Earthquake Response of a Tall Building Proceedings. 3rd World Conference on Earthquake Engineering, Vol. II, Wellington, New Zealand.
5. TIMOSHENKO, S., and GOODIER, J. N. (1951): Theory of Elasticity. McGraw-Hill, p. 277.

Summary

In earthquake resistant design it is customary to calculate the dynamic properties of a proposed structure as part of the procedure used to establish the seismic design loads. Recent developments of inelastic analysis techniques using a digital computer enable the elasto-plastic response to strong motion earthquakes to be investigated.

The problems encountered in applying elastic and elasto-plastic seismic analysis procedures to a multispan railway bridge are described and the results obtained are presented.

Résumé

Le calcul des propriétés dynamiques des structures fait habituellement partie du processus d'établissement de la résistance aux charges sismiques. Les développements récents des techniques d'analyses non-élastiques utilisant un calculateur digital permettent l'examen de la réaction élasto-plastique à des secousses sismiques violentes.

Les problèmes rencontrés dans l'application des procédés d'analyse sismique élastique et élasto-plastique à un pont de chemin de fer à arches multiples sont décrits et les résultats obtenus sont présentés.

Zusammenfassung

Beim Entwurf von erdbebensicheren Bauten berechnet man ihre dynamischen Eigenschaften gewöhnlich als Teil des für die Feststellung der seismischen Widerstandsfähigkeit angewandten Verfahrens. Die neuesten Entwicklungen in der Verwendung von Digital-Elektronenrechner für die nichtelastische Analyse ermöglichen die Untersuchung der elasto-plastischen Reaktion auf starke Erdbeben.

Die Probleme, die bei der Anwendung der elastischen und elasto-plastischen seismischen Berechnungsverfahren auf eine mehrfeldrige Eisenbahnbrücke auftreten, werden im folgenden beschrieben und die erzielten Ergebnisse dargestellt.